Hot-Deformation Mechanisms in Near-Alpha Titanium Alloy 685

V. Gopala Krishna, Y.V.R.K. Prasad, N.C. Birla, and G. Sambasiva Rao

Using a dynamic materials model, processing and instability maps have been developed for a near-α titanium alloy 685 with low oxygen content in the temperature range of 775–1,025 °C and a strain-rate range of 0.001–10 s^{-1} with a view to optimizing its hot workability. This grade undergoes dynamic recrystallization with a peak efficiency of 55 percent at 975 °C and 0.001 s^{-1}, which are the optimum parameters for hot working. Even though in conventional near-α titanium alloys the process of dynamic recrystallization is not reported, its occurence in this particular grade is attributed to lower oxygen concentration, which may help in grain-boundary migrations required for the occurrence of the process.

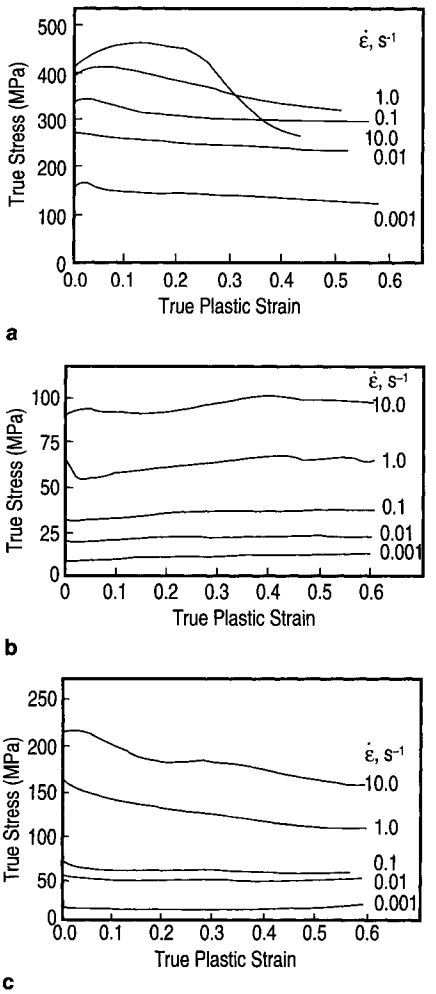

Figure 1. Typical true stress-strain curves of low-oxygen alloy 685 at (a) 825°C, (b) 975°C, and (c) 1,025°C at various strain rates.

INTRODUCTION

Mechanical processing is an important step in the manufacture of engineering components; with improved instrumentation of these processing techniques, it has become easier to execute complicated shapemaking processes with the utmost precision. However, sophistication in the instrumentation alone cannot ensure a defect-free, metallurgically sound product and control of the product's microstructure during mechanical processing is required. Workability is greatly influenced by the temperature of deformation, strain rate, and state-of-stress.[1]

There are several specialized tests to measure hot workability, including the axisymmetric hot-compression test.[2] The stress-state during the test is very similar to many bulk deformation processes. The problems of necking (e.g., tension) or material reorientation (e.g., torsion) are not encountered, therefore, deformation to a very large extent is possible before fracture. The extent of barreling can be minimized by the application of lubricants between specimen ends and compression platens. Thus, the hot-compression test is unique for workability evaluation.

Titanium alloy 685 (Ti-6.5Al-5Zr-0.5Mo-0.25Si), a near-α alloy, is characterized by a predominantly α-phase microstructure, which has been shown to be associated with its highest creep resistance at temperatures up to 520°C.[3] The near-α characteristics of this alloy permit hot working and heat treatment in the β-phase field without embrittlement risk. Excessive time at β-temperatures leads to undesirable grain coarsening, adversely affecting ductility. In contrast, forging can also be carried out in an α + β field without any loss of tensile or creep strength, as compared with β-processed material. However, in this case, initial working is carried out in the β-field, and subsequent reduction of at least 2:1 is made in the α–β range. Thus, the forging route should aim to provide a material that, on subsequent treatment in the β field, recrystallizes to a fine, uniform, β-grain structure.

To obtain control of these characteristics, hot-deformation behavior over wide temperature and strain-rate changes must be established. The hot-deformation characteristics of similar titanium alloys have been studied earlier.[1,4,5] Although practical limits of working temperatures are set by excessive grain growth and surface contamination caused by absorption of interstitial elements (i.e., O_2 and N_2[6,7]), literature is silent

Table I. Flow Stress Data at Various Strain Rates and Temperatures*

Strain	Strain Rate (s^{-1})	Temperature 775°C	825°C	875°C	925°C	975°C	1,025°C
0.1	0.001	248.9	152.2	114.4	47.6	17.7	9.9
	0.010	367.0	262.1	193.6	88.6	50.7	21.0
	0.100	569.0	328.4	245.2	122.6	61.8	32.5
	1.000	649.5	475.9	341.7	316.4	163.4	57.0
	10.000	603.4	502.2	409.1	385.5	226.5	140.8
0.2	0.001	244.3	148.1	109.2	46.9	16.0	10.9
	0.010	355.3	256.1	186.6	86.0	49.0	22.5
	0.100	530.9	311.4	233.1	144.8	62.0	35.2
	1.000	665.2	460.0	320.9	285.1	149.5	60.0
	10.000	612.3	498.6	386.2	355.3	204.9	133.1
0.3	0.001	234.2	144.9	103.7	47.3	15.9	11.0
	0.010	347.0	251.6	183.3	84.1	47.6	21.4
	0.100	482.1	304.5	227.6	110.6	61.1	35.5
	1.000	575.7	418.5	300.2	263.7	139.8	62.5
	10.000	436.8	383.4	349.8	326.3	200.5	135.3
0.4	0.001	227.9	138.9	101.3	46.0	14.9	10.5
	0.010	336.7	243.2	178.6	83.2	46.6	21.0
	0.100	440.8	303.2	224.5	107.6	57.4	35.5
	1.000	535.1	390.0	281.8	248.5	130.8	62.5
	10.000	194.3	249.0	309.9	285.3	186.6	133.2
0.5	0.001	215.2	132.0	94.8	44.3	15.5	10.5
	0.010	325.1	237.6	172.3	81.0	44.9	20.2
	0.100	421.9	297.9	218.0	103.6	54.3	34.9
	1.000	568.7	384.8	265.0	233.4	124.2	63.2
	10.000	26.8	122.6	292.1	259.9	173.0	126.7

* Corrected for adiabatic temperature increase.

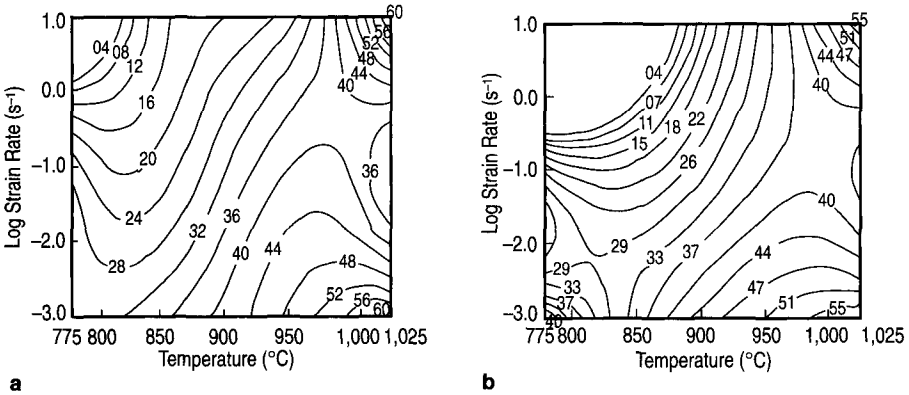

Figure 2. Power dissipation maps for low-oxygen alloy 685 at strains of (a) 0.2 and (b) 0.4. The number against each contour indicates the effiiciency percent.

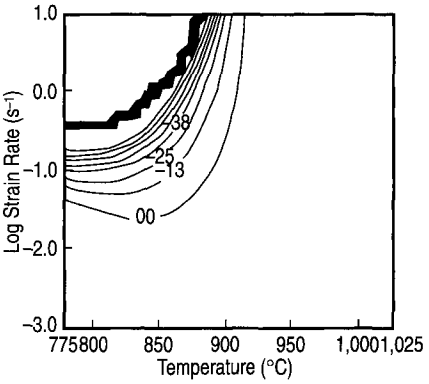

Figure 3. A contour map showing instability on the temperature-strain-rate plane.

on the deformation behavior of alloy 685 with a low oxygen level. The development of processing maps for evaluating the hot-deformation behavior of alloy 685 with a low-oxygen content has been selected for use in this investigation because it gives the range of temperature and strain rate at which the particular alloy can be processed.

Processing maps are developed on the basis of a dynamic materials model.[8–10] In this model, the workpiece deforming under hot-working conditions is considered to be a dissipater of power. At any instant, the power dissipation occurs through a temperature rise (G content) and a microstructural change (J content). The factor that partitions the power is the strain-rate sensitivity (m) of the flow stress σ. At a given temperature and strain, J is given by[6]

$$J = \frac{\sigma\dot{\varepsilon}m}{m+1} \qquad (1)$$

Where $\dot{\varepsilon}$ is the strain rate. The value of J for a nonlinear dissipater is normalized with that of a linear dissipater (m = 1) to obtain a dimensionless parameter called the

EXPERIMENTAL PROCEDURES

The chemical composition of alloy 685 used in this investigation is Ti-6.27Al-5.03Zr-0.44Mo-0.205Si with 655 ppm O_2 and 61 ppm H. The starting material, supplied by Midhani, Hyderabad, was in β-forged condition. The initial microstructure consisted of a slightly deformed acicular α (transformed β) and prior β grain boundaries along with a few grains of primary α (light) as seen in Figure A. Cylindrical specimens of 8 mm ϕ, 12 mm height were machined from the starting material. Concentric grooves of about 0.5 mm depth were engraved on both of the faces of the specimen to facilitate the retention of lubricant. A chamber of 1 mm at 45° was machined along the edges of the faces to avoid foldover in the initial stages of compression. A 0.5 mm die hole with a depth of 5 mm was also made at mid-height of the specimen for insertion of a thermocouple.

Hot-compression tests were carried out on a computer-controlled, servo-hydraulic testing machine with a load capacity of ±100 kN. It can control the movement of its actuator from 0.003 mm/s up to 1,200 mm/s, with a stroke length of 50 mm. A linear-variant displacement transducer was used to record instantaneous actuator position, wherein a microprocessor signal controls the actuator speed in such a way that it is always directly proportional to the specimen height at that particular instance. The specimens were compressed between two platens made up of superalloy IN 100.

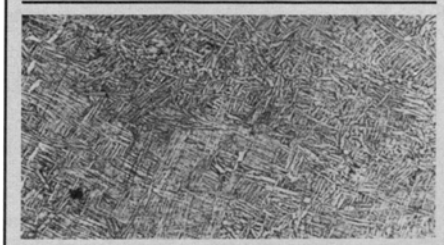

Figure A. The microstructure of alloy 685.

The entire setup was kept in a resistance heating furnace, and the required testing temperature was maintained within ±2°C. Specimen temperature was monitored with the help of a Chromel-Alumel thermocouple embedded in the hole provided in the sample. This thermocouple also helped in measuring the adiabatic temperature rise in the specimen through an oscilloscope. Testing temperatures ranged from 775–1,025°C with strain rates of 0.001 s^{-1}, 0.01 s^{-1}, 0.1 s^{-1}, 1 s^{-1}, and 10 s^{-1}. In each case, the specimens were compressed to about half their height (0.5 strain). Prior to hot-compression testing, a borosilicate-glass powder (delta glaze) coating was applied to the specimens to act not only as a lubricant but also as a protective coating against oxidation at the test temperatures.

The load-stroke data obtained from compression tests were processed in a Micro-Vax computer, and true stress-strain curves were plotted. The flow-stress data obtained at different temperatures and strain rates were corrected for the adiabatic temperature rise. Using flow-stress data, power dissipation maps were constructed based on a dynamic materials model at different strains. Instability maps as a function of temperature and strain rate were also plotted to understand regimes of flow instabilities.

After deformation, selected specimens were sectioned vertically at the center (parallel to the compression axis) by an Isomet precision low-speed saw and were prepared for metallographic examination using standard procedures. The specimens were etched with Kroll's reagent. Some specimens with temperature and strain rates within the domains were examined for microstructural features in a 300 kV Phillips 430T transmission electron microscope. Thin slices of specimens were mechanically polished to about 0.1 mm thickness followed by preparation of foils by twin-jet electropolishing. A six percent sulfuric acid in methanol solution was used as a polishing reagent, and the temperature of polishing was maintained at ≅ –45°C.

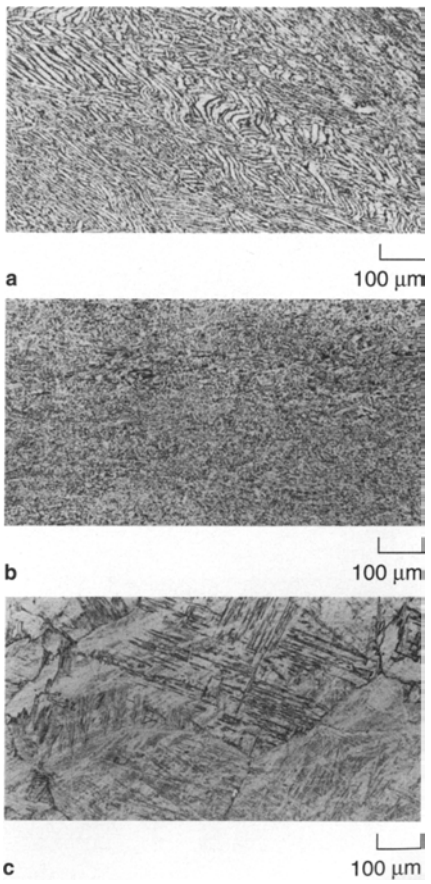

Figure 4. The microstructures of deformed specimens at a strain rate of 0.001 s^{-1} at (a) 875°C, (b) 925°C, and 1,025°C.

Figure 5. A TEM of a specimen deformed at 1,025°C and a strain rate of 0.001 s^{-1}.

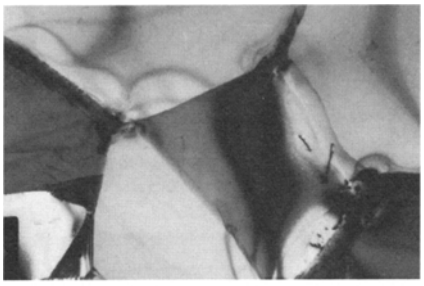

Figure 6. A TEM of a specimen deformed at 975°C and a strain rate of 0.001 s^{-1}.

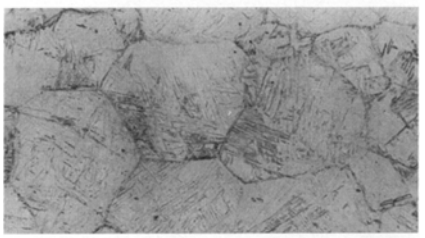

Figure 7. The microstructure of a specimen deformed at 1,025°C and a strain rate of 10 s^{-1}.

Figure 8. A TEM of the specimen deformed at 1,025°C and a strain rate of 10 s^{-1}.

efficiency of power dissipation.

$$\eta = \frac{J}{J_{max}} = \frac{2m}{(m+1)} \quad (2)$$

The variation of η with temperature and strain rate constitutes a processing map, which exhibits various domains that may be correlated with specific microstructural mechanisms. The processing maps may be superimposed with a criterion for the occurrence of microstructural instabilities given by[1,11,12]

$$\varsigma(\dot{\varepsilon}) = \frac{\delta \ln[m/(m+1)]}{\delta \ln \dot{\varepsilon}} + m < 0 \quad (3)$$

Where $\varsigma(\dot{\varepsilon})$ is negative, microstructural instabilities (e.g., in the form of flow localization) will appear. The regimes of instabilities must be avoided in processing the materials.

RESULTS

True stress-strain curves, plotted as a function of strain rate at 825°C, 975°C, and 1,025°C are shown in Figure 1. Flow-stress data obtained at different temperatures, strain rates, and strains corrected for the adiabatic temperature increase are given in Table I. The true stress-strain curves exhibited, in general, a much larger degree of flow softening at all test temperatures as well as higher strain rates;[6] steady-state behavior is established at strain rates of 0.1 s^{-1} and below.

Typical power dissipation maps obtained at 0.2 strain and 0.4 strain are presented in Figure 2. The maps at other strains are similar, indicating that the effect of strain is not significant. These maps exhibit two domains above 850°C at strain rates lower than 0.1 s^{-1} as well as above 1 s^{-1} with peak efficiency of about 55–60%. The efficiency in these two domains decreases with increasing strain and is about 55% at a strain of 0.4. An instability map showing the contours of the efficiency parameters $\varsigma(\varepsilon)$ on the temperature-strain rate plane for 0.4 strain is shown in Figure 3. The regime for which $\varsigma(\dot{\varepsilon})$ is negative (Equation 3), represents flow instability; the instability region for the alloy under investigation lies below 875°C and above 0.03 s^{-1}.

DISCUSSION

Conventional alloy 685 normally has an oxygen content of 1,200–1,500 ppm and a β-transus temperature at 1,020 ± 10°C.[3] The alloy under investigation has a much lower oxygen content (655 ppm), and, therefore, the β-transus temperature is lowered to ≅980°C, since oxygen is a well-known α-stabilizer.

Interpretation of the Processing Maps

The processing domain, occurring at strain rates lower than 0.1 s^{-1}, shows a change in the curvature of contours around the β-transus temperature. In order to identify the process occurring in this domain, microstructural examination of specimens deformed at 875°C, 925°C, 975°C, and 1,025°C with a strain rate of 0.001 s^{-1} was conducted. Microstructures obtained are shown in Figure 4. Specimens deformed at 925°C and 975°C (Figure 4b) exhibited spheroidization of the acicular α structure present in the starting specimen. The microstructure obtained on the specimen deformed at 875°C (Figure 4a) has partial features of spheroidization. A specimen deformed at 1,025°C (Figure 4c) exhibited a transformed β-microstructure, since this temperature is above β-transus. A transmission electron micrograph (TEM) of this specimen also shows transformed β platelets (Figure 5). On the other hand, a TEM of a specimen deformed at 975°C under this domain exhibited recrystallized grain structure within pre-existing β-grain boundaries (Figure 6).[13]

The microstructural observations clearly indicate that the lower strain rate domain represents spheroidization of acicular transformed β microstructure. It may be termed as a process of dynamic recrystallization (DRX), where shear stress cuts the laths and reconstitutes in the form of spheroids for minimizing interface energy. This type of DRX has high efficiency of the order of 55%, as observed earlier in other titanium alloys—Ti6242[14] and α_2 titanium aluminides.[15] Under these conditions, stress-strain curves exhibit flow softening (Figure 1b), since shear stress promotes a greater degree of spheroidization.

In conventional near-α alloys, the DRX process is not reported. Instead, a process of superplasticity occurs under these conditions, which is often used for the manufacture of components by isothermal forging. It should be noted that the present observation of the DRX process is specific for the material under investigation and may be attributed to the lower oxygen level present in the alloy. It is likely that the lower oxygen concentrations may help in grain-boundary migrations, which are required for the occurrence of DRX.

The domain occurring at 1,025°C and strain rates above 1 s^{-1} has an efficiency of about 55% (Figure 2b). At these temperatures, β-phase is stable and undergoes DRX as seen from the microstructures obtained on the specimens deformed at 1,025°C and 10 s^{-1} (Figure 7). In contrast, the microstructure of the specimen deformed at 1,025°C

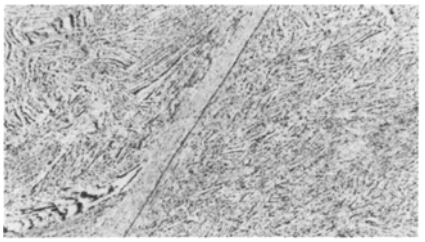

100 μm

Figure 9. The microsctructure of the specimen deformed at 825°C and a strain rate of 10 s^{-1}. The compression axis is almost 45° to the length of the crack.

ABOUT THE AUTHORS

V. Gopala Krishna earned his master's degree in metallurgical engineering at Kakatiya University, India, in 1984. He is currently joint regional director of the Regional Centre for Military Airworthiness (Materials), Ministry of Defence, Defence Research and Development Organization, India.

Y.V.R.K. Prasad earned his Ph.D. in metallurgical engineering at the Indian Institute of Science, Bangalore. He is a professor in the Department of Metallurgical Engineering at the Indian Institute of Science, Bangalore.

N.C. Birla earned his Ph.D. in metallurgical engineering at the University of Cincinnati in 1972. He is director, grade II, at the Defence Metallurgical Research Laboratory, Ministry of Defence, Defence Research and Development Organization, India.

G. Sambasiva Rao earned his Ph.D. in metallurgical engineering at the Indian Institute of Science, Bangalore. He is a professor in the Department of Metallurgical Engineering at the Regional Engineering College, Warangal.

For more information, contact V. Gopala Krishna, Defence Research Development Organization, Ministry of Defence, Regional Centre for Military Airworthiness, P.O. Kanchanbagh, Hyderabad 500 058, India; telephone (91) 842-4-239749; fax (91) 842-4-218827.

and 0.001 s^{-1} has a very large grain size (Figure 4c). A TEM (Figure 8) of the specimen deformed at 1,025°C and 10 s^{-1} exhibited intense dislocation structures in the α-platelets.[16]

On the basis of these microstructural observations, high-strain-rate domain may be interpreted to represent DRX of β-phase. Stress-strain behavior under these conditions is steady-state with some uneven oscillations (Figure 1c).[17] It is likely that this domain may not occur if the oxygen content is higher (i.e., >650 ppm).

Manifestation of Instabilities

The material exhibits flow instabilities at strain rates higher than 0.03 s^{-1} and temperatures below 875°. Microstructural examination of the specimen deformed at 825°C and 10 s^{-1} (Figure 9) clearly exhibited adiabatic shear bands.[18,19,20] These shear bands are oriented at about 45° to the compression axis. Since shear bands are often associated with material elements and not spatial or geometry-related directions, their directions rotate away from the compression axis once they are initiated and get further rotated with increased strain or decreased temperature.[21] It may be noted that the intense shear localization has resulted in fine cracking along this band and, thus, a very fine-grain transformed microstructure along the crack length. This regime of instability may be avoided in processing the material.

ACKNOWLEDGEMENTS

V. Gopala Krishna expresses his gratitude to the Regional Center for Military Airworthiness (Materials), Hyderabad, for giving permission for this article; Midhani and Aeronautical Materials Testing Laboratory, Hyderabad, for the supply of the material and the machining of samples; and Defence Metallurgical Research Laboratory, Hyderabad and Indian Institute of Science, Bangalore, for the provision of research facilities in carrying out the present investigation work.

References

1. Y.V.R.K. Prasad, *Indian Jr. of Tech.*, 28 (August 1990), pp. 435–451.
2. G.E. Dieter, *ASM Metals Handbook—Forming and Forging*, vol. 14 (Metals Park, OH: ASM, 1987).
3. *Ti-alloy IMI 685* brochure (U.K.: Imperial Metal Industries)
4. P. Dadras and J.F. Thomas, Jr., *Metall. Trans. A*, 12A (1981), pp. 1867–1876.
5. S.L. Semiatin, J.F. Thomas, Jr., and P. Dadras, *Metall. Trans. A*, 14A (1983), p. 2363.
6. S.L. Semiatin and G.D. Lahoti, *Metall. Trans. A*, 12A (October 1981), pp. 1705–1717.
7. S.L. Semiatin and G.D. Lahoti, *Metall. Trans. A*, 13A (1982), pp. 275–288.
8. Y.V.R.K. Prasad et al., *Metall. Trans. A*, 15A (1984), pp. 1883–1892.
9. H.L. Gegel et al., *ASM Metals Handbook–Forming and Forging*, vol. 14 (Metals Park, OH: ASM, 1987), pp. 417–438.
10. J.M. Alexander, *Modelling of Hot Deformation of Steels*, ed. J.C. Lenard (Berlin: Springer-Verlag, 1984), pp. 101–114.
11. H. Ziegler, "Some Extremum Principles in Irreversible Thermodynamics with Application to Continuum Mechanics," *Progress in Solid Mechanics*, vol. 4, ed. I.N. Sneddon and R. Hill (Amsterdam, North-Holland, 1963), pp. 93–193.
12. A.K.S. Kalyan Kumar, "Criteria for Predicting Metallurgical Instabilities in Processing," M.Sc (Engg.) thesis, I.I.Sc, Bangalore, India (1987).
13. S.E. Ion, F.J. Humphreys, and S.H. White, *Acta. Metall.*, 30 (1982), pp. 1909–1919.
14. Y.V.R.K. Prasad et al., *Met. Trans. A*, 15A (October 1984), pp. 1883–1892.
15. P.K. Sagar, D. Banerjee, and Y.V.R.K. Prasad, *Mat. Sci. Engrg. A*, 177 (1994), pp. 185–197.
16. W. Roberts, *Deformation Processing and Structure*, ed. G. Krauss (Metals Park, OH: ASM, 1984), p. 109.
17. M.J. Luton and C.M. Sellars, *Acta. Metall.*, 17 (1969), p. 1033.
18. C.M. Young and O.D. Sherby, "Metal Forming—Inter Relation Between Theory and Practice," *Metal Forming-Inter Relation Between Theory and Practice*, ed. A.L. Hoffmanner (New York: Plenum Press, 1971), p. 429.
19. G.L. Wulf, *Int. J. Mech. Sci.*, 21 (1979), p. 713.
20. F.N. Lake and D.J. Moracz, tech. report AFML-TR-71-112, TRW, Inc., Cleveland, OH (May 1971).
21. A.K. Chakrabarti and J.W. Spretnak, *Metall. Trans. A*, 6 (1975), p. 733.